PCCP

COMMUNICATION

In situ investigation of dye adsorption on TiO$_2$ films using a quartz crystal microbalance with a dissipation technique†

Hauke A. Harms,[a] Nicolas Tétreault,[a] Viktoria Gusak,[b] Bengt Kasemo*[b] and Michael Grätzel*[a]

Dye adsorption plays a crucial role in dye-sensitized solar cells. Herein, we demonstrate an *in situ* liquid-phase analytical technique to quantify in real time adsorption of dye and coadsorbates on flat and mesoporous TiO$_2$ films. For the first time, a molar ratio of co-adsorbed Y123 and chenodeoxycholic acid has been measured.

Dye sensitized solar cells (DSCs) provide a viable alternative to traditional semiconductor solar cells in that they have the potential to harvest solar energy with high efficiency and at low environmental and industrial costs.[1] They are based mainly on cheap and nontoxic materials, are roll-to-roll compatible and offer short energy payback times.[2] To date the highest certified power conversion efficiency (PCE) for a DSC using iodide/triiodide (I_3^-/I^-) electrolytes and a ruthenium dye is 11.4% although Yella *et al*. have recently achieved 12.3% using a Co$^{(II/III)}$tris(bipyridyl)-based redox electrolyte in conjunction with a donor–π–bridge–acceptor (D–π–A) zinc porphyrin dye as sensitizer and Y123 as cosensitizer.[3–6]

At the heart of the DSC is a self-assembled monolayer (SAM) of dye molecules adsorbed on a high surface area mesoporous TiO$_2$ photoanode and infiltrated with an electrolyte containing the redox shuttle molecule. Dye loading has been found to be crucial for the DSC performance in three complementary ways. First, the amount of the dye adsorbed on the TiO$_2$ surface and its extinction coefficient determine the fraction of sunlight that can be harvested, which in turn affects the cell's photocurrent (J_{sc}). Second, the photo-excited dye has to efficiently inject electrons into the semiconductor and must be regenerated by the redox mediator in the electrolyte. For these processes to be efficient, it is mandatory to have only a monolayer of dye on the surface and avoid multilayer buildup through aggregation.[5] Third, the dye monolayer must act as a blocking layer that prevents recombination between the injected charge in the semiconductor and the oxidized form of the redox couple in the electrolyte. In addition,

the recombination rate has been shown to decrease significantly when using molecular coadsorbates like dineohexyl bis-(3,3-dimethyl-butyl)-phosphonic acid or chenodeoxycholic acid (cheno).[7,8] The blocking layer becomes particularly important when using Co^{2+}/Co^{3+} or spiro-OMeTAD which offer higher redox potential but suffer from faster recombination rates than the two-electron (I_3^-/I^-) redox couple.[6,9]

Co-sensitization using multiple dyes of complementary spectral absorption has been shown to be a promising approach to improve PCE but is not yet fully understood.[10] In addition to the combined optical absorption of the two dyes there is a reported "concerto effect", which is likely to be related to rearrangement of the dye molecules on the TiO$_2$ surface, as well as to the formation of a more effective recombination barrier. These results highlight the need for a better understanding of the dye adsorption dynamics as well as an optimization of the SAM of dye. However, most studies are limited to optical absorption on mesoporous substrates, and a more direct method is necessary to quantify the effect on dye loading of dye and additive concentrations, solvent composition, pH, temperature and adsorption–desorption cycling.[11]

Herein, we demonstrate a new *in situ* liquid-phase analytical technique to quantify the amount, saturation time and adsorption kinetics of dye uptake on flat and mesoporous TiO$_2$ films using a quartz microbalance with dissipation technique (QCM-D). By directly measuring mass uptake, we can monitor sub-monolayers of adsorbates independently of their optical properties, which renders the QCM-D technique unique for its capability to quantify not only dye, but also coadsorbates on flat films. Moreover, sensitivity is high enough to obtain quantitative measurements on flat surfaces enabling for the first time the investigation of the actual adsorption process, independently of the diffusion in the mesoporous film. This clear separation allows for model systems that will help understand fundamental processes in state-of-the-art DSCs. The technique is first demonstrated by precise measurements of Z907Na and Y123 mass uptake on atomic layer deposited (ALD) flat TiO$_2$, and then on a mesoporous nanoparticle film directly deposited on the quartz crystal, where the signal increased by two orders of magnitude.‡ The mass uptake measured was found to be in good agreement with quantities obtained by complementary optical fluorescence measurements. To the best of our knowledge, this constitutes the first *in situ* measurement of the adsorption of a sensitizer on a flat

[a] *Laboratory of Photonics and Interfaces, École Polytechnique Fédérale de Lausanne, 1015 Lausanne, Switzerland.*
  E-mail: michael.graetzel@epfl.ch
[b] *Chemical Physics Group, Department of Applied Physics, Chalmers University of Technology, 412 96 Göteborg, Sweden.*
  E-mail: kasemo@chalmers.se

† Electronic supplementary information (ESI) available: QCM-D data on different ratios of ^{t}BuOH : MeCN in Z907 dye solution, FTIR data on adsorbed ^{t}BuOH, complete QCM-D data on Y123 and cheno, blank on mesoporous film. See DOI: 10.1039/c2cp41268c

This journal is © the Owner Societies 2012

Phys. Chem. Chem. Phys., 2012, **14**, 9037–9040 | 9037

TiO₂ film that is unrestricted by dye diffusion in the mesoporous structure. To take further advantage of the potential of the QCM-D technique, we determine the ratio between cheno and Y123 when coadsorbed on a flat film, which is the first quantification of this kind.

QCM-D measurements have been developed and used extensively in a variety of fields, *e.g.*, biomolecule adsorption, lipid membranes, polymer and corrosion science and cell–surface interactions for the last 15 years.[12–14] The operation principle is that of a conventional quartz crystal microbalance, measuring the shift of an electro-acoustic resonance frequency upon mass loading. We use an E4 instrument from Q-Sense, where the sensor is mounted in a temperature controlled chamber and exposed to a constant flow of solvent or dye solution on one side. Different solutions can be flowed through the chamber, starting with a reference solution that will be used as a baseline for the frequency shift, followed by sample solutions containing the species of interest. Measured frequency shifts depend on the adsorbed mass, the viscosity of the overlying (bulk) liquid and the viscoelastic properties of the adsorbed layer. Besides the fundamental resonance at 5 MHz, the QCM-D apparatus also measures overtones up to 65 MHz and their energy dissipation (or damping), see ESI.† In the measurements presented here, the dissipation is constant during exposure to each of the reference or Z907 solutions used, falling back to its initial value upon rinsing. This confirms that the adsorbates form a thin rigid layer on the TiO₂ substrate, vindicating the use of the Sauerbrey equation that directly relates the frequency shift Δf to the mass uptake per unit area, Δm. In the case of our sensor this is given by $\Delta m = -17.5 \, \Delta f \, n^{-1}$ Hz ng cm^{-2}, where n is the overtone number. Unless mentioned otherwise, all figures in this study display the normalized shift of the 7th overtone at 35 MHz. The quartz crystal sensors (QSX-301) were coated by ALD with a 65 nm thick TiO₂ film that had an initial RMS roughness of 0.27 nm on a 40 nm frame (by AFM). The sensor is mounted in a flow chamber (40 μl size) with its TiO₂ side in contact with the liquid pumped through at a rate of 100 μl min^{-1}.

The red curve in Fig. 1(a) shows the most simple case of dye uptake against a reference solution of *tert*-butanol : acetonitrile (*t*BuOH : MeCN) 1 : 1 mixture, which is the same solvent used for the dye (55 μM Z907 in *t*BuOH : MeCN mixture). In this configuration, frequency shift relates to mass uptake only, not to viscosity changes, since the influence of the latter is constant through the measurement. During the first 3 min of the 30 min exposure, the frequency decreases rapidly followed by a much slower shift, indicating at least two different adsorption phases. Upon rinsing for 30 min, there is 15–20% desorption of the total uptake. The second exposure results in a fast uptake of an amount similar to what was desorbed in the preceding rinsing period. The final (2nd) rinsing results in qualitatively the same behaviour as for the first one, apart from slower desorption upon rinsing attaining a slightly lower plateau. The latter corresponds to a small additional mass uptake during the second exposure that is likely due to a rearrangement within the SAM during the first rinsing, leading to a densification of the dye monolayer upon the second exposure.

The experiment shown in Fig. 1(b) and all subsequent measurements employed plain acetonitrile (MeCN) as a reference solvent.
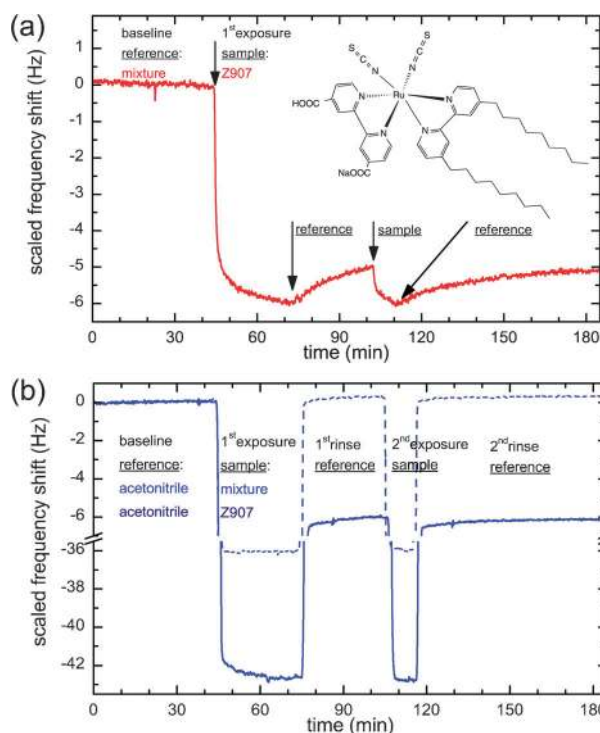

Fig. 1 Frequency shift *versus* time upon two subsequent Z907Na dye exposures against different references and blank measurement on a flat TiO₂ film. (a) 55 μM Z907 in *t*BuOH : MeCN (1 : 1) against a *t*BuOH : MeCN (1 : 1) reference (red line). (b) 44 μM Z907 in *t*BuOH : MeCN (1 : 1) against a plain MeCN reference (solid blue), the dashed blue is the blank *t*BuOH : MeCN (1 : 1) against a plain MeCN reference.

The rational for this choice is that the latter is commonly used for rinsing TiO₂ films after dye loading during the preparation of DSCs, reducing dye desorption due to the lower solubility of Z907 in pure MeCN than in the *t*BuOH : MeCN mixture. The dashed blue line in Fig. 1(b) shows a blank measurement of *t*BuOH : MeCN mix against a MeCN reference. Here, the frequency shift relates almost exclusively to bulk viscosity, and upon rinsing with MeCN, the frequency shift returns to zero within an error of 0.2 Hz. However, both solvent molecules do adsorb on the surface, and *t*BuOH remains even after rinsing, see Fig. S3 in the ESI.† Although their ratio cannot be obtained, the fact that the baseline is not affected indicates that both species have the same area weight. The solid blue line in Fig. 1(b) shows an exposure to a 44 μM Z907 solution (in *t*BuOH : MeCN mixture) against a MeCN reference. When switching from a MeCN reference solution to a Z907 dye solution (blue), the dye will attach to the surface with both of its –COOH groups, replacing two MeCN molecules.[15,16] The rest of the TiO₂ underneath the dye will remain covered with solvent molecules.[17] Moreover, MeCN molecules may be replaced by *t*BuOH molecules, which will not change the area weight. The observed frequency shift during exposure is due to simultaneous bulk viscosity change and dye adsorption. After 20 min of exposure, the shift has reached a plateau, indicating the presence of a monolayer of molecules on the surface. During rinsing with the MeCN reference the frequency shifts rapidly back due to the change of viscosity of the solvent, but little desorption is observed. After the second exposure, desorption is even less

9038 | *Phys. Chem. Chem. Phys.*, 2012, **14**, 9037–9040

This journal is © the Owner Societies 2012

pronounced and occurs over a longer time period. The final frequency shift (6.2 Hz) is 5% larger than the shift after the first exposure (5.9 Hz), indicating a small additional mass uptake, as was also observed in Fig. 1(a). This is ascribed again to a molecular rearrangement within the SAM during the first rinsing and a densification of the dye molecule film upon the second exposure. The difference of about 20% in the final frequency shift between the red and the blue curve in Fig. 1 is mainly due to better solubility and thus desorption of the dye in the mixture.

Measurements for different dye concentrations are shown in Fig. 2. The inset shows frequency shifts *versus* time for a flat TiO$_2$ film for two subsequent exposures of 30 min and 10 min to Z907 dye solution of concentrations from 0.0 μM to 45.0 μM in a ^{t}BuOH : MeCN (1 : 1) mixture, using plain MeCN as a reference. There is a clear increase of absolute final frequency shift with increasing concentration, as well as an increase of the adsorption rate (slope) during the first exposure. The outer Fig. 2 shows the absolute frequency shift Δf_{eq} after 60 min rinsing with the reference solution as a function of the concentration of the dye solution. Red squares represent the same data as shown in the inset, while blue squares are from an analogous dataset obtained for two subsequent 10 min exposures. The red curve is a fit with a Langmuir isotherm $\Delta f_{eq} = (\Delta f_{max})K_{eq,Z907}c_{Z907}/(1 + K_{eq,Z907}c_{Z907})$ where Δf_{max} is the final frequency shift for full coverage with a monolayer, $K_{eq,Z907}$ is the equilibrium adsorption constant and c_{Z907} is the Z907 dye concentration in MeCN : ^{t}BuOH. While the Langmuir equation describes our data well, the validity of the specific assumptions underlying this model for the present case may be questioned. However, we still pursue this analysis in order to compare with literature data. Fitting the points in the concentration range from 0.0 μM to 65.0 μM gives $K_{eq,Z907} = 5.1 \pm 0.3 \times 10^6$ M^{-1} and $\Delta f_{max} = 5.9 \pm 0.3$ Hz. From the Sauerbrey equation this corresponds to an area mass of 103 ng cm^{-2} yielding a Z907 concentration of 1.27×10^{-10} mol cm^{-2} assuming a flat surface at full monolayer coverage, based on its molecular weight MW$_{Z907Na}$ = 892 g mol^{-1} and MW$_{MeCN}$ = 41 g mol^{-} for MeCN. This in turn gives a projected area of 1.31 nm^2 per molecule. To confirm that the frequency shift is truly caused by

the dye itself, it was desorbed from the TiO$_2$-surface after the QCM-D measurement using a solution of tetrabutylammonium hydroxide in dimethylformamide. The dye concentration was quantified by comparing its fluorescence signal against a reference solution leading to a projected area of 1.26 nm^2 per molecule in excellent agreement with the value derived from the QCM-D experiments. These values are also close to the area of 1.6 nm^2 determined for the N719 dye whose structure is similar to that of Z907.[18]

The formal equilibrium adsorption constant $K_{eq,Z907} = 5.1 \times 10^6$ M^{-1} is higher than previously published equilibrium adsorption constants for similar ruthenium dyes. Studies on N719 dye adsorption[19] in nanoparticle dispersions find a $K_{eq,N719} = 0.12 \times 10^6$ M^{-1} when sensitizing from an ethanol solution. This is attributed to the difference in the dye structures affecting their solubility and mode of interaction with the TiO$_2$ surface. Finally, it should be noted that for the Z907 concentration of 250 μM, normally used for staining porous films in state-of-the-art DSCs, the frequency shift for dye uptake on a flat film is only 5.5 Hz, that is 0.4 Hz less than Δf_{max} above.

Fig. 3(a) shows QCM-D data for the organic D–π–A dye Y123 (green line) and for coadsorption of Y123 + cheno (orange line). During the gap on the time axis there is a 30 min plus 10 min exposure, see ESI.† Here, only the final frequency shift is displayed.
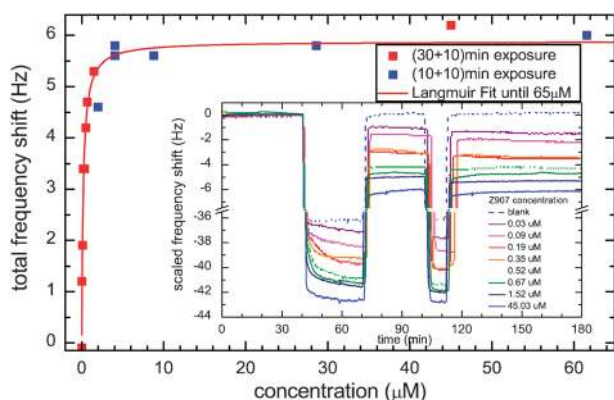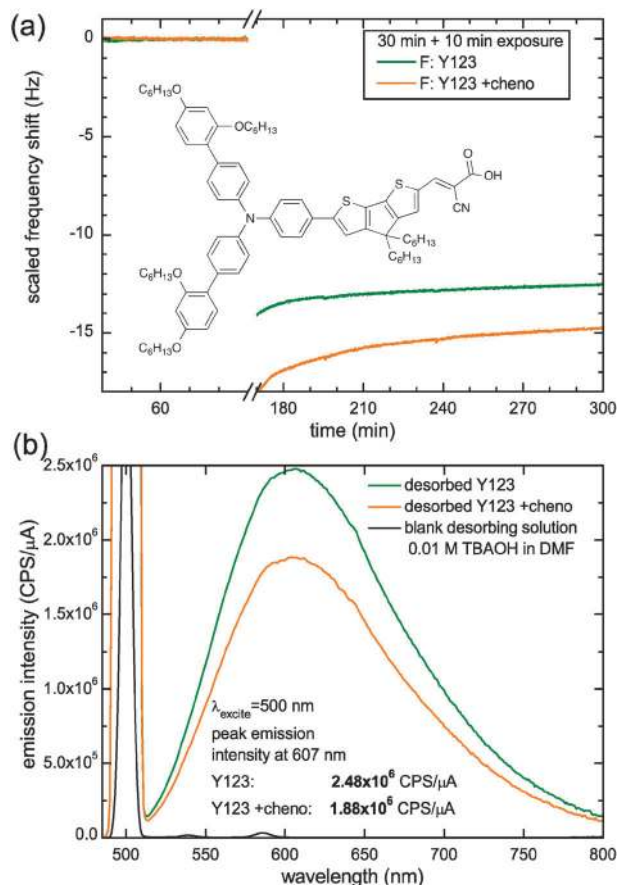

Fig. 2 Inset: frequency shift upon two subsequent Z907 exposures for different concentrations of dye. Exposures of 30 min and 10 min with Z907 concentrations from 0 μM to 45 μM in ^{t}BuOH : MeCN (1 : 1) against a plain MeCN reference. Outer figure: final frequency shift as a function of dye concentration and formally fitted Langmuir adsorption isotherm (red curve).

Fig. 3 Adsorption of organic D–π–A dye Y123 (0.1 mM) with or without coadsorbate cheno (5.0 mM) in ^{t}BuOH : MeCN (1 : 1) against a MeCN reference. (a) Final frequency shift after 30 min plus 10 min exposure (during break). (b) Fluorescence emission intensity after desorbing the dye from the QCM-D sensor.

The frequency shift of -12.7 Hz for Y123 corresponds to a mass uptake of 222 ng cm^{-2}. Assuming a flat substrate and an effective molecular weight of $MW_{Y123} - MW_{MeCN} = 1196$ g mol^{-1}, we calculate a coverage of 1.86×10^{-10} mol cm^{-2}, corresponding to an area of 0.9 nm^2 per molecule in a dense monolayer. The orange line in Fig. 3(a) shows the final frequency shift after exposure to 0.1 mM Y123 + 5.0 mM cheno in ^{t}BuOH : MeCN (1 : 1). For further analysis Y123 and Y123 + cheno were desorbed from the sensors after the QCM-D measurement and their fluorescence emission intensities were compared, see Fig. 3(b). From the 24% decrease in fluorescence observed for the Y123 + cheno sample, one can infer that cheno reduces the Y123 surface concentration by the same percentage. Since both Y123 and cheno bind to the surface *via* one carboxylic acid, coadsorption results in a decrease in dye uptake. Taking this into account for the mass uptake, we calculate that of the 15.0 Hz shift measured for Y123 + cheno, only 9.7 Hz can be attributed to Y123 and 5.3 Hz to cheno. Assuming a thin rigid film on a flat surface, this corresponds to a coverage of 1.42×10^{-10} mol cm^{-2} for Y123 and 2.63×10^{-10} mol cm^{-2} for cheno, corresponding to a molar ratio of 1 : 1.7 for Y123 to cheno when both are coadsorbed at the surface.

Fig. 4 shows QCM-D measurements on a 2 μm thick mesoporous TiO$_2$ film screen-printed directly onto the sensor, displaying dye loading from a 250 μM Z907 dye solution in ^{t}BuOH : MeCN (1 : 1) against a MeCN reference. The dark blue line is the frequency shift for the 15 MHz QCM resonance, which shows a final frequency shift of 10^3 Hz that relates to molecules adsorbed during exposure. The ratio between adsorption-related signal and bulk liquid-related signal is 1000 : 50, compared to a ratio of 6 : 40 as observed for flat films. Note also the much longer time scale compared to the flat film. The light blue line is the frequency response of the 55 MHz overtone. Although the behaviour of the frequency shifts for the mesoporous samples will need further analysis to extract all the contained information, we have strong indications that the observed frequency shifts on mesoporous films are due to three effects: mass uptake, bulk viscosity change, and a change of fluid dynamics inside the mesoporous film related to pore size diminution by adsorbed molecules. From measurements on thicker films up to 10 μm, we can estimate that the shear wave amplitude decays completely within the first 2 μm of the mesoporous film. Further QCM-D measurements on mesoporous TiO$_2$ films will be subject to a separate study.

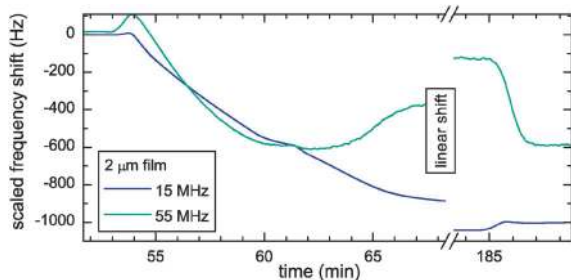**Fig. 4** Dye loading on 2 μm thick mesoporous TiO$_2$ films: Z907 exposure, 0.25 mM in ^{t}BuOH : MeCN (1 : 1) against a MeCN reference, showing different overtones at 15 or 55 MHz.

In conclusion, we demonstrated a new *in situ* liquid-phase analytical technique to quantify the amount, saturation time and kinetics of dye uptake on flat and mesoporous TiO$_2$ films using a quartz microbalance with dissipation technique. Future studies will entail fundamental investigations into surface rearrangements of the adsorbed dye monolayer, including high resolution microscopy. Furthermore, the loading of mesoporous films and the possibility to monitor nano-scale fluid dynamics will be explored with respect to possible sensing applications as well as its relevance for dye-sensitized solar cells.

Acknowledgements

Notes and references

‡ Abbreviations: Z907, *cis*-RuLL′(SCN)$_2$ (L = 4,4′-dicarboxylic acid-2,2′-bipyridine, L′ = 4,4′-dinonyl-2,2′-bipyridine); Y123, 3-{6-{4-[bis(2′,4′-dihexyloxybiphenyl-4-yl)amino]phenyl}-4,4-di-hexyl-cyclopenta-[2,1-*b*:3,4-*b*′]dithiophene-2-yl}-2-cyanoacrylic acid.

1 B. O'Regan and M. Grätzel, *Nature*, 1991, **353**, 737–740.
2 H. Greijer, L. Karlson, S. Lindquist and A. Hagfeldt, *Renewable Energy*, 2001, **23**, 27–39.
3 L. Han, A. Islam, H. Chen, C. Malapaka, S. Zhang, X. Yang and M. Yanagida, *Energy Environ. Sci.*, 2012, **5**, 6057–6060.
4 F. Gao, Y. Wang, D. Shi, J. Zhang, M. Wang and X. Jing, *J. Am. Chem. Soc.*, 2008, **130**, 10720–10728.
5 M. Grätzel, *Prog. Photovoltaics*, 2006, **14**, 429–442.
6 A. Yella, H. W. Lee, H. N. Tsao, C. Yi, A. K. Chandiran, M. K. Nazeeruddin, E. W. G. Diau, C. Y. Yeh, S. M. Zakeeruddin and M. Grätzel, *Science*, 2011, **334**, 629–634.
7 M. Wang, X. Li, H. Lin, P. Pechy, S. M. Zakeeruddin and M. Graetzel, *Dalton Trans.*, 2009, 10015–10020.
8 X. Ren, Q. Feng, G. Zhou, C.-H. Huang and Z.-S. Wang, *J. Phys. Chem. C*, 2010, **114**, 7190–7195.
9 U. Bach, D. Lupo, P. Comte, J. E. Moser and F. Weissörtel, *Nature*, 1998, **395**, 583–585.
10 R. Y. Ogura, S. Nakane, M. Morooka, M. Orihashi, Y. Suzuki and K. Noda, *Appl. Phys. Lett.*, 2009, **94**, 073308.
11 G. Bazzan, J. R. Deneault, T.-S. Kang, B. E. Taylor and M. F. Durstock, *Adv. Funct. Mater.*, 2011, **21**, 3268–3274.
12 M. Rodahl, F. Hook, A. Krozer, P. Brzezinski and B. Kasemo, *Rev. Sci. Instrum.*, 1995, **66**, 3924–3930.
13 A. Domack, O. Prucker, J. Rühe and D. Johannsmann, *Phys. Rev. E*, 1997, **56**, 680–689.
14 M. Voinova, M. Rodahl, M. Jonson and B. Kasemo, *Phys. Scr.*, 1999, **59**, 391–396.
15 M. Suzuki and T. Ami, *Mater. Sci. Eng., B*, 1996, **41**, 166–173.
16 M. K. Nazeeruddin, R. Humphry-Baker, P. Liska and M. Grätzel, *J. Phys. Chem. B*, 2003, **107**, 8981–8987.
17 F. Schiffmann, J. VandeVondele, J. Hutter, R. Wirz, A. Urakawa and A. Baiker, *J. Phys. Chem. C*, 2010, **114**, 8398–8404.
18 V. Shklover, Y. E. Ovchinnikov, L. S. Braginsky, S. M. Zakeeruddin and M. Grätzel, *Chem. Mater.*, 1998, **10**, 2533–2541.
19 J. Fan, W. Cai and J. Yu, *Chem.–Asian J.*, 2011, **6**, 2481–2490.